# Precision Model Independent Determination of $|V_{ub}|$ from $B \to \pi l \nu$

Christian M. Arnesen,[1] Benjamin Grinstein,[2] Ira Z. Rothstein,[3] and Iain W. Stewart[1]

[1]*Center for Theoretical Physics, Massachusetts Institute of Technology, Cambridge, Massachusetts 02139, USA*
[2]*Department of Physics, University of California, San Diego, La Jolla, California, 92093, USA*
[3]*Department of Physics, Carnegie Mellon University, Pittsburgh, Pennsylvania 15213, USA*

(Received 3 May 2005; published 12 August 2005)

A precision method for determining $|V_{ub}|$ using the full range in $q^2$ of $B \to \pi \ell \nu$ data is presented. At large $q^2$ the form factor is taken from unquenched lattice QCD, at $q^2 = 0$ we impose a model independent constraint obtained from $B \to \pi\pi$ using the soft-collinear effective theory, and the shape is constrained using QCD dispersion relations. We find $|V_{ub}| = (3.54 \pm 0.17 \pm 0.44) \times 10^{-3}$. With 5% experimental error and 12% theory error, this is competitive with inclusive methods. Theory error is dominated by the input points, with negligible uncertainty from the dispersion relations.

DOI: 10.1103/PhysRevLett.95.071802 PACS numbers: 12.15.Hh, 13.20.He

The remarkable success of the $B$ factories has led to a new era for precision results in the Cabibbo-Kobayashi-Maskawa (CKM) sector of the standard model. For $|V_{ub}|$ measurements must now surmount the dominant theoretical uncertainties. For inclusive semileptonic decays measuring $|V_{ub}|$ is difficult because cuts either make observables sensitive to a structure function that demands input from radiative decays or require neutrino reconstruction. The heavy flavor averaging group (HFAG)'s average from inclusive decays based on operator product expansion (OPE) techniques is $10^3|V_{ub}| = 4.7 \pm 0.4$ [1]. For $|V_{ub}|$ from $B \to \pi \ell \bar{\nu}$, model independent form factor information relies on precision lattice QCD.

Recently, the Fermilab/MILC [2] and HPQCD [3] groups have presented unquenched lattice results for $B \to \pi$ form factors. Uncertainties in the discretization restrict the kinematics to pions that are not too energetic $E_\pi \lesssim 1$ GeV, for which the invariant mass of the lepton pair is $15 \lesssim q^2 \lesssim 26.4$ GeV$^2$. For $\bar{B}^0 \to \pi^+ \ell \bar{\nu}$, $d\Gamma/dq^2 = N|V_{ub}|^2 |\vec{p}_\pi|^3 |f_+(q^2)|^2$, where $N = G_F^2/(24\pi^3)$, so, unfortunately, since the phase space goes as $|\vec{p}_\pi|^3$, there are fewer events and more experimental uncertainty in this region. For example, Belle [4] found $10^3|V_{ub}|_{q^2 \geq 16} = 3.87 \pm 0.70 \pm 0.22^{+0.85}_{-0.51}$ with [2] and $4.73 \pm 0.85 \pm 0.27^{+0.74}_{-0.50}$ with [3] where the errors are statistical, systematic, and theoretical. In quadrature this is an uncertainty of $\sim$25%.

The latest *BABAR,* CLEO, and Belle average is [5]

$$\mathrm{Br}(\bar{B}^0 \to \pi^+ \ell^- \bar{\nu}) = (1.39 \pm 0.12) \times 10^{-4}, \qquad (1)$$

which should yield $|V_{ub}|$ at the $\approx 5\%$ level. So far extractions of $|V_{ub}|$ from the total Br rely on QCD sum rules [6] and quark models for input. HFAG reports results on $\mathrm{Br}(B \to \{\pi, \rho, \omega\} \ell \bar{\nu})$ that lead to central values $10^3|V_{ub}| =$ 2.9 to 3.9 [1]. Because of the uncertainty they do not currently average over exclusive extractions of $|V_{ub}|$.

In this Letter we present a model independent exclusive method for determining the entire $B \to \pi$ form factor $f_+(q^2)$ and thus $|V_{ub}|$. A total uncertainty $\delta|V_{ub}| \approx 13\%$ is achieved by combining (1) the unquenched lattice results [2,3], (2) a constraint at $q^2 = 0$ derived from soft-collinear effective theory (SCET) [7] and $B \to \pi\pi$ data, which determines $|V_{ub}| f_+(0)$, and (3) dispersion relations and analyticity that allow us to interpolate over the entire region of $q^2$ by bounding the shape of $f_+(q^2)$ between input points [8,9]. The SCET constraint induces an additional implicit functional dependence on $|V_{ub}|$ in the form factors. Our first analysis uses just the total Br, yielding an analytic formula for $|V_{ub}|$. The second includes $q^2$ spectra with a $\chi^2$ minimization that allows the experimental data to constrain the theoretical uncertainty. A different approach for including the $q^2$ spectra was developed in [10] based on the Lellouch distribution method [11].

*Analyticity bounds.*—We briefly review how analyticity constrains the $B \to \pi$ form factors, $f_+$ and $f_0$, referring to [8,9,12] for more detail. Our notation follows [12], and we set $t_\pm = (m_B \pm m_\pi)^2$. Suitable derivatives of a time ordered product of currents, $\Pi^{\mu\nu}(q^2) = i \int d^4x e^{iqx} \langle 0|T J^\mu(x) J^\dagger(0)|0\rangle$, can be computed with an OPE in QCD and are related by a dispersion relation to moments of a positive definite sum over exclusive states

$$\mathrm{Im}\, \Pi^{\mu\nu} = \int [\mathrm{p.s.}] \langle 0|J^{\dagger\nu}|\bar{B}\pi\rangle \langle \bar{B}\pi|J^\mu|0\rangle + \cdots. \qquad (2)$$

Keeping this first term bounds a weighted integral over $t_+ \leq t \leq \infty$ of the squared $B\pi$ production form factor. Using analyticity and crossing symmetry, this constrains the shape in $t = q^2$ of the form factors for $B \to \pi$ in the physical region $0 \leq t \leq t_-$. The results are simple to express by writing each of $f_+(t)$ and $f_0(t)$ as a series,

$$f(t) = \frac{1}{P(t)\phi(t, t_0)} \sum_{k=0}^{\infty} a_k(t_0) z(t, t_0)^k, \qquad (3)$$

with coefficients $a_k$ that parametrize different allowed functional forms. The variable

$$z(t, t_0) = \frac{\sqrt{t_+ - t} - \sqrt{t_+ - t_0}}{\sqrt{t_+ - t} + \sqrt{t_+ - t_0}} \qquad (4)$$

 

maps $t_+ < t < \infty$ onto $|z| = 1$ and $-\infty < t < t_+$ onto $z \in [-1, 1]$. $t_0$ is a free parameter that can be chosen to attain the tightest possible bounds, and it defines $z(t_0, t_0) = 0$. We take $t_0 = 0.65 t_-$ giving $-0.34 \le z \le 0.22$ for $t$ in the $B \to \pi$ range. In Eq. (3) the "Blaschke" factor $P(t)$ eliminates subthreshold poles, so $P(t) = 1$ for $f_0$, while $P(t) = z(t; m_{B^*}^2)$ for $f_+$ due to the $B^*$ pole. Finally, the "outer" function is given by

$$\phi(t, t_0) = \sqrt{\frac{n_I}{K \chi_J^{(0)}}} (\sqrt{t_+ - t_0} + \sqrt{t_+ - t_0}) \frac{(t_+ - t)^{(a+1)/4}}{(t_+ - t_0)^{1/4}} \times \frac{(\sqrt{t_+ - t} + \sqrt{t_+ - t_-})^{a/2}}{(\sqrt{t_+ - t} + \sqrt{t_+})^{(b+3)}}, \quad (5)$$

where $n_I = 3/2$ and for $f_+$: $[K = 48\pi, a = 3, b = 2]$, while for $f_0$: $[K = 16\pi/(t_+ t_-), a = 1, b = 1]$. Here $\chi_J^{(0)}$ is obtained from derivatives of $\Pi(q^2)$ computed with an OPE. At two loops in terms of the pole mass and condensates and taking $\mu = m_b$ [11,13]

$$\chi_{f_+}^{(0)} = \frac{3[1 + 1.140\alpha_s(m_b)]}{32\pi^2 m_b^2} - \frac{\bar{m}_b \langle \bar{u}u \rangle}{m_b^6} - \frac{\langle \alpha_s G^2 \rangle}{12\pi m_b^6},$$
$$\chi_{f_0}^{(0)} = \frac{[1 + 0.751\alpha_s(m_b)]}{8\pi^2} + \frac{\bar{m}_b \langle \bar{u}u \rangle}{m_b^4} + \frac{\langle \alpha_s G^2 \rangle}{12\pi m_b^4}, \quad (6)$$

with $\bar{m}_b \langle \bar{u}u \rangle \simeq -0.076$ GeV$^4$, $\langle \alpha_s G^2 \rangle \simeq 0.063$ GeV$^4$. We use $m_b^{\rm pole} = 4.88$ GeV as a central value. With Eq. (3) the dispersive bound gives a constraint on the coefficients

$$\sum_{k=0}^{n_{\max}} a_k^2 \le 1, \quad (7)$$

for any choice of $n_{\max}$.

Equations (3) and (7) give only a weak constraint on the normalization of the form factor $f_+$. In particular, data favor $a_0 \sim 0.02$, so $a_0^2 \ll 1$. The main power of analyticity is that if we fix $f_+(q^2)$ at $n_{\max}$ input points then it constrains the $q^2$ shape between these points. With $n_{\max} = 5$ the error from the bounds is negligibly small relative to other uncertainties, as we see below (our analysis is also insensitive to the exact values of $\chi_J^{(0)}$ or $m_b$). The bounds can be strengthened using heavy quark symmetry or higher moments [12], but since this uncertainty is very small we do not use these improvements.

*Input points.*—A constraint at $q^2 = 0$ is useful in pinning down the form factor in the small $q^2$ region. Here we implement a constraint at $q^2 = 0$ on $|V_{\rm ub}| f_+(0)$ that follows from a $B \to \pi\pi$ factorization theorem derived with SCET [7]. The result holds in QCD and uses isospin symmetry and data to eliminate effects due to the relative magnitude and strong phase of penguin contributions. Manipulating formulas in [7], the result is

$$|V_{\rm ub}| f_+(0) = \left[ \frac{64\pi}{m_B^3 f_\pi^2} \frac{{\rm Br}(B^- \to \pi^0 \pi^-)}{\tau_{B^-} |V_{\rm ud}|^2 G_F^2} \right]^{1/2} \times \left[ \frac{(C_1 + C_2) t_c - C_2}{C_1^2 - C_2^2} \right], \quad (8)$$

up to corrections of order $\alpha_s(m_b)$ and $\Lambda_{\rm QCD}/m_b$. Here $C_1 = 1.08$ and $C_2 = -0.177$ are parameters in the electroweak Hamiltonian at $\mu = m_b$ (we drop the tiny $C_{3,4}$), and $t_c$ is a hadronic parameter whose deviation from 1 measures the size of color suppressed amplitudes. In terms of the angles $\beta$, $\gamma$ of the unitarity triangle and $CP$ asymmetries $S_{\pi^+\pi^-}$ and $C_{\pi^+\pi^-}$ in $B \to \pi^+\pi^-$,

$$t_c = \sqrt{\bar{R}_c \frac{(1 + B_{\pi^+\pi^-} \cos 2\beta + S_{\pi^+\pi^-} \sin 2\beta)}{2 \sin^2 \gamma}}, \quad (9)$$

with $\bar{R}_c = [{\rm Br}(B^0 \to \pi^+\pi^-)\tau_{B^-}]/[2{\rm Br}(B^- \to \pi^0\pi^-)\tau_{B^0}]$ and $B_{\pi^+\pi^-} = (1 - C_{\pi^+\pi^-}^2 - S_{\pi^+\pi^-}^2)^{1/2}$. Equations (8) and (9) improve on relations between $B \to \pi\pi$ and $B \to \pi \ell \bar{\nu}$ derived earlier, such as in Ref. [14], because they do not rely on expanding in $\alpha_s(\sqrt{m_b \Lambda})$ or require the use of QCD sum rules for input parameters to calculate $t_c$.

Using the latest $B \to \pi\pi$ data [1], Eq. (8) gives

$$f_{\rm in}^0 = |V_{\rm ub}| f_+(0) = (7.2 \pm 1.8) \times 10^{-4}. \quad (10)$$

This estimate of 25% uncertainty accounts for the 10% experimental uncertainty, and ~20% theory uncertainty from perturbative and power corrections. The experimental uncertainty includes $\gamma = 70^\circ \pm 15^\circ$, which covers the range from global fits, and that preferred by the SCET based $B \to \pi\pi$ method from Ref. [15]. As noted in [7], the dependence of $|V_{\rm ub}| f_+(0)$ on $\gamma$ is mild for larger $\gamma$'s. Estimates for perturbative and power corrections to Eq. (8) are each at the ~10% level even when "chirally enhanced" terms are included [14,16].

Next we consider lattice QCD input points, $f_{\rm in}^k$, which are crucial in fixing the form factor normalization. The staggered fermion $({\rm det}M)^{1/4}$ trick might add model dependence, but we take the agreement with data in [17] to indicate that this is small. References [2,3] find consistent results with different heavy quark actions. As our default we use [2] since they have a point at larger $q^2$:

$$f_{\rm in}^1 = f_+(15.87) = 0.799 \pm 0.058 \pm 0.088,$$
$$f_{\rm in}^2 = f_+(18.58) = 1.128 \pm 0.086 \pm 0.124, \quad (11)$$
$$f_{\rm in}^3 = f_+(24.09) = 3.262 \pm 0.324 \pm 0.359.$$

The first errors in (11) are statistical, $\pm\sigma_i$, and the second are 11% systematic errors, $\pm y f_{\rm in}^i$, with $y = 0.11$. For the lattice error matrix, we use $E_{ij} = \sigma_i^2 \delta_{ij} + y^2 f_{\rm in}^i f_{\rm in}^j$, which takes $\sigma_i$ uncorrelated and includes 100% correlation in the systematic error. Of the 11 reported lattice points, we use only three at separated $q^2$. This maximizes the shape information while minimizing additional correlations that may occur in neighboring points.

Chiral perturbation theory (ChPT) gives model independent input for $f_+$ (and $f_0$) when $E_\pi \sim m_\pi$, namely,

$$f_+(q^2(E_\pi)) = \frac{g f_B m_B}{2 f_\pi (E_\pi + m_{B^*} - m_B)} \left[ 1 + \mathcal{O}\left( \frac{E_\pi}{\Delta} \right) \right], \quad (12)$$

where $g$ is the $B^* B \pi$ coupling and $f_B$ the decay constant.

Possible pole contributions from the low lying $J^\pi = 0^+, 1^+, 2^+$ states vanish by parity and angular momentum conservation. The first corrections scale as $E_\pi/\Delta$, where $\Delta \sim 600$ MeV is the mass splitting to the first radially excited $1^-$ state above the $B^*$. We take $g = 0.5$. Using heavy quark symmetry, this is compatible with $\Gamma(D^{*+})$ and $D^*$ Br ratios; updating the ChPT fit in [18] gives $g_{D_* D_\pi} \simeq 0.51$ (at an order with no counterterm operators or $1/m_c$ corrections absorbed in $g$). For the lattice average Ref. [19] gives $f_B = 189$ MeV. Thus,

$$f^4_{\rm in} = f_+(26.42) = 10.38 \pm 3.63, \tag{13}$$

where this fairly conservative 35% error is from uncertainty in $gf_B$, and from the $m_\pi/\Delta \sim 23\%$ corrections.

*Determining $f_+$.*—To determine $f_+(t)$ we drop $a_{k\geq 6}$ in Eq. (3), and take $a_5 \to a_5(1-z^2)^{-1/2}$, which properly bounds the truncation error [20]. The $f^{0-4}$ input points then fix $a_{0-4}$ as functions of $a_5$. Functions that bound $f_+(t)$ are determined from the maximum and minimum values of $a_5$ satisfying (7) with $n_{\rm max} = 5$. Thus we solve

$$\begin{aligned} 18.3a_0 + 3.96a_1 + 0.857a_2 + 0.185a_3 + 0.0401a_4 + 0.008\,87a_5 &= f^0/|V_{\rm ub}|, \\ 37.8a_0 + 0.960a_1 + 0.0244a_2 + 0.000\,619a_3 + 1.57\times 10^{-5}a_4 + 4.00\times 10^{-7}a_5 &= f^1, \ldots, \\ 304.0a_0 - 103.6a_1 + 35.3a_2 - 12.0a_3 + 4.10a_4 - 1.49a_5 &= f^4, \qquad a_0^2 + a_1^2 + a_3^2 + a_4^2 + a_5^2 = 1. \end{aligned} \tag{14}$$

In Eq. (3) this yields two solutions, $F_\pm$, with parameters

$$f_+(t) = F_\pm(t, \{f_0/|V_{\rm ub}|, f_1, f_2, f_3, f_4\}). \tag{15}$$

To see how well these solutions bound the form factor, we fix $|V_{\rm ub}| = 3.6\times 10^{-3}$, $f^i = f^i_{\rm in}$, and plot the bounds as the two black solid lines in Fig. 1. The curves lie on top of each other. For comparison we show dashed lines for the bounds on $f_+$ and $f_0$ obtained using four lattice points (shown as dots). With these inputs the constraint $f_+(0) = f_0(0)$ is less effective than using the SCET point.

*$|V_{\rm ub}|$ from total* Br *fraction.*—Equating Eq. (1) with the theoretical rate obtained using Eq. (15) gives an analytic equation for $|V_{\rm ub}|$. With $f^i = f^i_{\rm in}$ the solution is

$$|V_{\rm ub}| = (4.13 \pm 0.21 \pm 0.58)\times 10^{-3}. \tag{16}$$

The first error is experimental, 5.2%, propagated from Eq. (1). The second error, 14%, is from theory and is broken down in Table I. It is dominated by the input points. The bound uncertainty from the choice of solution is $<1\%$ (but would grow to $\pm 12\%$ without the SCET point). The error from $m_b$ and the order in the OPE and are very small

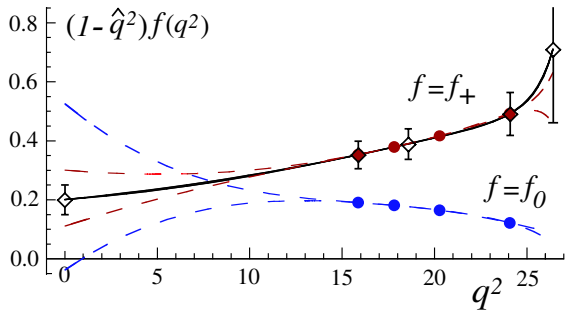


FIG. 1 (color online). Upper and lower bounds on the form factors from dispersion relations, where $\hat{q}^2 = q^2/m^2_{B^*}$. The overlapping solid black lines are bounds $F_\pm$ derived with the SCET point, 3 lattice points, and the ChPT point (diamonds with error bars). The dashed lines are the bounds derived using instead four lattice points (shown by the dots). Input point errors are not included in these lines, and are analyzed in the text.

because shifts in the normalization through $\chi^{(0)}_{f_+}$ are compensated by shifts in the $a_n$ coefficients, except for the last term $a_5$, which gives a small contribution. To ensure consistency with the dispersion bounds the input point uncertainty is calculated using the Lellouch method of generating random points from Gaussians [11], giving $10^3|V_{\rm ub}| = (3.96 \pm 0.20 \pm 0.56)$. Our distributions were determined using Eqs. (10), (11), and (13) and the correlation matrix $E_{ij}$. Taken individually the SCET and ChPT points give $\sim 5\%$ error, so the lattice uncertainty dominates.

*$|V_{\rm ub}|$ from $q^2$ spectra.*—Results for partial branching fractions $({\rm Br}^{\rm exp}_i \pm \delta{\rm Br}_i)$ over different bins in $q^2$ are also available. CLEO [21] and BELLE [4] present results for 3 bins with untagged and $\pi^+$ semileptonic tags, respectively. *BABAR* [5] recently presented total rates from hadronic and leptonic $\pi^+$ and $\pi^0$ tags as well as $\pi^+$ semileptonic tagged data in 3 bins and untagged data over 5 bins. By fitting to these 17 pieces of data with MINUIT, we exploit the $q^2$ shape information. To do this, we define

$$\begin{aligned} \chi^2 = &\sum_{i,j=1}^{3} [f^i_{\rm in} - f^i][f^j_{\rm in} - f^j](E^{-1})_{ij} + \frac{[f^0_{\rm in} - f^0]^2}{(\delta f^0)^2} \\ &+ \frac{[f^4_{\rm in} - f^4]^2}{(\delta f^4)^2} + \sum_{i=1}^{17} \frac{[{\rm Br}^{\rm exp}_i - {\rm Br}_i(V_{\rm ub}, F_\pm)]^2}{(\delta {\rm Br}_i)^2}, \end{aligned} \tag{17}$$

and minimize $\chi^2$ as a function of $|V_{\rm ub}|$ and $f^{0-4}$. $\chi^2$

TABLE I. Summary of theoretical uncertainties on $|V_{\rm ub}|$. Results are shown for an analysis from the total branching fraction, $\delta|V_{\rm ub}|^{\rm Br}$, and from using the $d\Gamma/dq^2$ spectrum, $\delta|V_{\rm ub}|^{q^2}$. For the input point error we quote the average from $F_\pm$.

| Type of error | Variation from | $\delta\lvert V_{\rm ub}\rvert^{\rm Br}$ | $\delta\lvert V_{\rm ub}\rvert^{q^2}$ |
|---|---|---|---|
| Input points | 1-$\sigma$ correlated errors | $\pm 14\%$ | $\pm 12\%$ |
| Bounds | $F_+$ versus $F_-$ | $\pm 0.6\%$ | $\pm 0.04\%$ |
| $m_b^{\rm pole}$ | $4.88 \pm 0.40$ | $\pm 0.1\%$ | $\pm 0.2\%$ |
| OPE order | 2 loop $\to$ 1 loop | $-0.2\%$ | $+0.3\%$ |

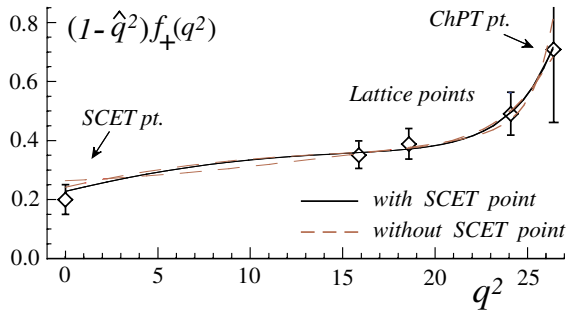


FIG. 2 (color online). Results from the $\chi^2$ fit of $|V_{ub}|$ and $f^{0-4}$ to the $q^2$ spectra ($\hat{q}^2 = q^2/m_{B^*}^2$). The two solid lines are obtained using either the $F_+$ or the $F_-$ solutions from Eq. (15). The two dashed lines repeat this analysis without using the SCET point.

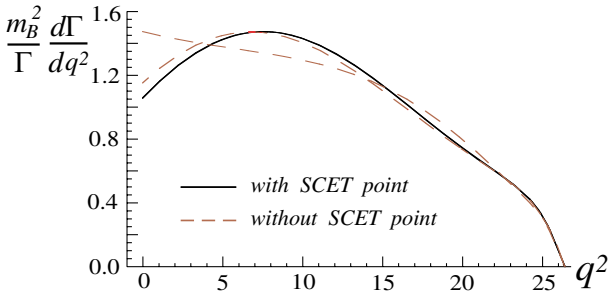


FIG. 3 (color online). The curves are as in Fig. 2, but for the decay rate.

contains both experimental and theoretical errors, with $E^{-1}$ the inverse error matrix. By allowing $f^{0-4}$ in $F_\pm$ to move away from $f_{\rm in}^{0-4}$, the theoretical rate is allowed to adjust itself based on the experimental $q^2$ shape.

Minimizing (17) gives $\chi^2/(\text{dof}) = 1.04$ and

$$|V_{ub}| = (3.54 \pm 0.47) \times 10^{-3}. \quad (18)$$

Results for $f_+(q^2)$ and $d\Gamma/dq^2$ are shown by the black solid curves in Figs. 2 and 3. Equation (18) has a total error of 13%. If we fix $f^{0-4} = f_{\rm in}^{0-4}$, then the experimental error is 4.9%, i.e., $\delta|V_{ub}| = \pm 0.17$. The remainder, $\delta|V_{ub}| = \pm 0.44$, is from the input points, so the $q^2$ spectra reduced the theory error to 12%. Other uncertainties are small as shown in Table I. The $q^2$ spectra favor a larger form factor between the lattice and SCET points, thus decreasing $|V_{ub}|$ from (16). Using Eqs. (10) and (13) this fit yields

$$f_+(0) = 0.227 \pm 0.047, \qquad g f_B = 96 \pm 29 \text{ MeV}, \quad (19)$$

consistent with our inputs. This $f_+(0)$ has 21% error.

Removing the SCET point $f^0$ from Eq. (17) leaves only semileptonic data and gives the fit shown by the dashed red lines in Figs. 2 and 3. The spectrum is now determined less precisely at small $q^2$, since these data bound only the area in the smallest $q^2$ bin. The result is $|V_{ub}| = (3.56 \pm 0.48) \times 10^{-3}$. It has the same input point error as Eq. (18) and a bit larger bound error, $\delta|V_{ub}| = 1.8\%$. Turning the use of Eq. (10) around, we can combine it with $f_+(0)$ to get an independent method for $|V_{ub}|$ from the nonleptonic data. The semileptonic fit gives $f_+(0) = 0.25 \pm 0.06$, so Eq. (10) yields $|V_{ub}|^{\rm nonlep} = (2.9 \pm 1.0) \times 10^{-3}$.

Our final result for $|V_{ub}|$ is given in (18). The final theory error is dominated by the lattice points, and is very close to their error. It will decrease with this error in the future. See also [22]. To go beyond the analysis here, it will be interesting to study the additional error correlation implied by the dispersion relations when lattice input points are included that are closer together.

We thank J. Branson, J. Flynn, L. Gibbons, A. Kronfeld, M. Okamoto, D. Pirjol, and J. Shigemitsu for helpful conversations. This work was supported by the U.S. Department of Energy under DOE-FG03-97ER40546 (B. G.), DOE-ER-40682-143 and DEAC02-6CH03000 (I. R.), the cooperative research agreement DF-FC02-94ER40818 and Office of Nuclear Science (C. A. and I. S.), and the DOE OJI program and the Sloan Foundation (I. S.). I. S. thanks the Institute of Nuclear Theory for their hospitality during the completion of this work.

[1] HFAG, http://www.slac.stanford.edu/xorg/hfag/.
[2] M. Okamoto *et al.* (Fermilab/MILC Collaboration), Nucl. Phys. B Proc. Suppl. **140**, 461 (2005).
[3] J. Shigemitsu *et al.* (HPQCD Collaboration), hep-lat/0408019.
[4] K. Abe *et al.* (Belle Collaboration), hep-ex/0408145.
[5] J. Dingfelder (*BABAR* Collaboration), contribution to CKM, 2005, http://ckm2005.ucsd.edu/WG/WG2/wed2/dingfelder-WG2-S1.pdf.
[6] P. Ball and R. Zwicky, Phys. Rev. D **71**, 014015 (2005); A. Khodjamirian *et al.*, Phys. Rev. D **62**, 114002 (2000).
[7] C. W. Bauer, D. Pirjol, I. Z. Rothstein, and I. W. Stewart, Phys. Rev. D **70**, 054015 (2004).
[8] C. Bourrely *et al.*, Nucl. Phys. **B189**, 157 (1981).
[9] C. G. Boyd, B. Grinstein, and R. F. Lebed, Phys. Rev. Lett. **74**, 4603 (1995); Nucl. Phys. **B461**, 493 (1996).
[10] M. Fukunaga and T. Onogi, Phys. Rev. D **71**, 034506 (2005).
[11] L. Lellouch, Nucl. Phys. **B479**, 353 (1996).
[12] C. G. Boyd and M. J. Savage, Phys. Rev. D **56**, 303 (1997).
[13] S. C. Generalis, J. Phys. G **16**, 367 (1990); **16**, 785 (1990).
[14] M. Beneke *et al.*, Nucl. Phys. **B591**, 313 (2000).
[15] C. W. Bauer *et al.*, Phys. Rev. Lett. **94**, 231802 (2005).
[16] C. W. Bauer *et al.*, hep-ph/0502094.
[17] C. Davies *et al.*, Phys. Rev. Lett. **92**, 022001 (2004).
[18] I. W. Stewart, Nucl. Phys. **B529**, 62 (1998).
[19] S. Hashimoto, hep-ph/0411126.
[20] C. G. Boyd and R. F. Lebed, Nucl. Phys. **B485**, 275 (1997).
[21] S. B. Athar *et al.* (CLEO Collaboration), Phys. Rev. D **68**, 072003 (2003).
[22] J. Flynn and J. Nieves (to be published). We thank J. Flynn for discussing his analysis with us prior to publication.